

## Modeling aerosols and extinction in the marine atmospheric boundary layer

G. de Leeuw, A.M.J. van Eijk and G.R. Noordhuis

TNO Physics and Electronics Laboratory  
P.O. Box 96864, 2509 JG The Hague, The Netherlands

### ABSTRACT

An analysis is presented of aerosol particle size distributions measured over the North Atlantic and extinction coefficients derived from these data. Two empirical models, an aerosol model and an extinction model, are formulated in terms of simple meteorological parameters (wind speed, relative humidity, air temperature and sea temperature). The choice of these parameters is based on considerations of their effects on the aerosol physics in the marine atmosphere. The performance of the models for predictions of the extinction coefficients at (laser) wavelengths in the visible and IR atmospheric windows is assessed. The results are compared with predictions of the Navy Aerosol Model (NAM).<sup>3,4</sup>

### 1. INTRODUCTION

The performance of electro-optic systems depends, among others, on the atmospheric conditions. Effects of the atmosphere on the transmitted radiation include the scattering and absorption by aerosols and gases, turbulence effects, and refraction caused by vertical gradients. In this contribution we address the effects of aerosols in the marine atmospheric boundary layer on the transmission in the atmospheric windows in the visible and IR wavelength bands. The parameter discussed is the extinction coefficient  $\alpha$ , which relates to the transmission  $T$  by:

$$T = \exp\left\{-\int_0^R \alpha(r) dr\right\}, \quad (1)$$

where  $R$  is the transmission path length between the electro-optic system and the target. The extinction coefficient  $\alpha$  may be a function of range due to atmospheric inhomogeneities. The extinction coefficient includes both scattering and absorption:

$$\alpha(r) = \alpha_{As}(r) + \alpha_{Aa}(r) + \alpha_{Ms}(r) + \alpha_{Ma}(r), \quad (2)$$

where the subscripts A and M denote aerosol and molecular contributions, respectively, to the scattering (s) and absorption (a). Molecular effects on the extinction coefficients will not further be considered here.

The atmosphere is transparent only in distinct bands in the visible, mid- and far-IR due to absorption by molecules. The transmission is further limited by the presence of aerosols. The concentrations of aerosols depend on the balance between production and removal, including advection effects. Over sea, the main source is sea spray that is generated when the wind causes wave breaking. (Photochemical processes generate mainly sub micron aerosol). The wind is also responsible for the generation of turbulence which transports the particles from the production zone near the air-sea interface, up into the boundary layer. Turbulence also has a large

effect on the deposition rate. Hence the wind speed plays a dominant role in the life cycle of the marine aerosol. Various other meteorological parameters influence the physics of the aerosol in the marine atmosphere. The relative humidity affects the size of the hygroscopic sea-salt particles due to their exchange of water vapor by evaporation and condensation. The air-sea temperature difference (ASTD), which determines the thermal stability, affects both the generation<sup>1</sup> and the transport of aerosol. The water temperature is believed to affect the production.<sup>1</sup> Wind direction and fetch determine the advection of aerosol of non-marine origin. Finally, the atmospheric vertical structure has an effect on vertical transport, exchanges at the top of the boundary layer and humidity effects as function of altitude.<sup>2</sup>

Models for the concentration of aerosols in the marine atmospheric boundary layer and their effects on extinction, usually describe the aerosol concentrations as function of these meteorological parameters. An example is the Navy Aerosol Model (NAM)<sup>3,4</sup> which is included in LOWTRAN.<sup>5</sup> NAM is also the kernel of the Naval Oceanic Vertical Aerosol Model (NOVAM).<sup>4,6,7</sup> The advantage of modeling the aerosol concentrations is that the physics of particles of different size and origin can be taken into account. In particular in complex coastal regions, where aerosols over the sea may originate both over land and from the sea, this approach is advantageous.<sup>8</sup>

Alternatively, the aerosol optical effects may be directly modelled as function of meteorological parameters. An example was presented by De Leeuw<sup>9</sup> for aerosol backscatter over the North Atlantic. That this approach is not generally successful was demonstrated in Van Eijk and De Leeuw<sup>10</sup> for extinction over the North Sea. Due to many near-by sources on land and the large differences in fetch, the aerosol composition varied greatly with wind direction (air mass trajectory),<sup>8</sup> and the aerosol extinction could not be directly correlated with wind speed.

Here we present an analysis of aerosol particle size distributions measured at the North Atlantic during a period of about one month. Based on this analysis, a model was formulated to forecast the aerosol extinction. Alternatively, the extinction coefficients were directly modelled as a function of meteorological parameters. An intercomparison of both approaches is made, as well as a comparison with NAM.

## 2. THE DATA BASE

Data were collected over the North Atlantic at Station Lima (57°N; 20°W), aboard the Dutch weather-ship Cumulus during a cruise from May 25 until June 28, 1983. The experiments are described by De Leeuw et al.<sup>16</sup> Particle size distributions in the 0.16-32  $\mu\text{m}$  diameter range were measured with PMS (Particle Measuring Systems, Boulder, CO, USA) optical particle counters ASAS-300-A and CSAS-100-HV, mounted on the deck at 12 m above the mean sea surface. The particle counters were manually pointed into the wind. The data were digitized and stored in the data acquisition system and transferred to a microcomputer at preset time intervals, via an IEEE interface. Particle concentrations  $\text{dN/dD}$  ( $\mu\text{m}^{-1}\cdot\text{cm}^{-3}$ ) were calculated for each size bin and polynomials of degree 2 and 5 were fitted to averaged particle size distributions in  $\log(\text{dN/dD})$  versus  $\log(D)$  space. The measurements were made 24 hours per day, except during rain. An exact Mie code was used to calculate extinction and backscatter coefficients at five (laser)wavelengths from the visible (0.55  $\mu\text{m}$ ) to the far-IR (10.6  $\mu\text{m}$ ). Extinction and backscatter coefficients at 1.064  $\mu\text{m}$  were directly measured with a lidar system. Visibility was recorded with an AEG point

visibility meter. Meteorological parameters were available from the weather-ship recordings. Since they were measured by instrumentation mounted at several heights, they were first corrected to the standard reference height of 10 m using the code of Liu et al.<sup>11</sup> Air mass characteristics are available from air mass trajectory analyses and Radon measurements. Impactor samples were used for chemical characterisation of the size-fractionated aerosol.

## 2.1 Data selection and validation

Before starting the analysis, aerosol data collected while sailing from the port of Rotterdam to Station Lima were removed from the data base because they were atypical for open-ocean conditions. Continental influences were clearly visible, both in the particle size distributions and in the chemical composition of impactor samples. South of Great Britain and Ireland, the northern wind advected continental particles causing an enhancement of the concentrations in the sub-micron range of about one order of magnitude. Sulphates dominated in this size fraction. As soon as we were clear of continental influences, the concentrations of sub-micron particles and sulphates were greatly reduced while the concentrations of giant particles consisting of sea-salt remained the same at this wind speed. This observation is another confirmation of the large influence of land on the aerosol in the marine atmosphere.

The purely marine character of the particle size distributions remaining in the data base was confirmed by the low Radon counts and the 72-hour air mass trajectories. The latter showed that the air masses encountered during this cruise had not been over land during the last three days before reaching Station Lima, except during a storm half-way the experiment.

The data base was further validated by removing clear spikes in time-serial plots. All measurements with RH>96% were disregarded in the analysis, because they had been made in fog, drizzle and rain. Such conditions are not representative for marine aerosol. Our data show that aerosol concentrations, extinction and backscatter coefficients rise fast under these conditions.

## 3. ANALYSIS

### 3.1 Aerosols

Following the procedure outlined by Van Eijk and De Leeuw,<sup>8</sup> the logarithms (base 10) of the aerosol concentrations  $C(D) = 10 \log(dN/dD)$  were parameterized in terms of meteorological parameters P. A two-step regression procedure was applied. In the first step a regression line

$$C(D)_{\text{fit}} = a + bP \quad (3)$$

with standard deviation  $\sigma$  and correlation coefficient cc was calculated. In the second step, regression was performed on only those data points which satisfy the Chauvenet criterion:<sup>12</sup>

$$C(D) - C(D)_{\text{fit}} < (1.42 + 0.301 \cdot \ln(N-4)) \cdot \sigma \quad (4)$$

where N is the total number of data points. In this way, outliers were removed from the fit. The validity of this procedure was justified afterward on the basis of case studies using air mass trajectories and synoptic weather maps. These case studies

should reasonably explain why a removed data point would behave different from the average.

**Humidity effects.** The changes in the particle size due to evaporation and condensation in response to changes in the relative humidity were taken into account by normalizing all concentrations  $C(D)$  at  $RH=80\%$ :<sup>13</sup>

$$C_{80}(D) = C(D') + {}^{10}\log g(S) \tag{5}$$

where  $C_{80}(D)$  denotes  $C(D)$ , normalized at  $RH=80\%$ , and  $D'$  represents the product of the diameter  $D$  and a dimensionless function  $g(S)$ :<sup>13</sup>

$$g(S) = 0.81 \{ \exp[0.066 S / (1.058 - S)] \} \tag{6}$$

In contrast to previous results from the analysis of the HEXMAX data set,<sup>8</sup> this correction is sufficient to remove any correlation of the aerosol concentrations with relative humidity. It is noted, however, that the weak correlations observed by Van Eijk and De Leeuw<sup>8</sup> after application of Fitzgerald's correction were caused by data at  $RH > 90\%$ . In the present data set, relative humidities were generally lower than  $90\%$ , except in cases with fog or precipitation which were excluded from the analysis.

**Wind speed.** The aerosol concentrations  $C_{80}(D)$  were correlated with  $u_{10N}$ , the wind speed at  $z=10$  m in neutral conditions. The concentrations of all particles in the size range from  $0.2-15 \mu\text{m}$  increase with wind speed, in contrast with the observations over the North Sea.<sup>8</sup> This is illustrated in Figure 1 for particles of

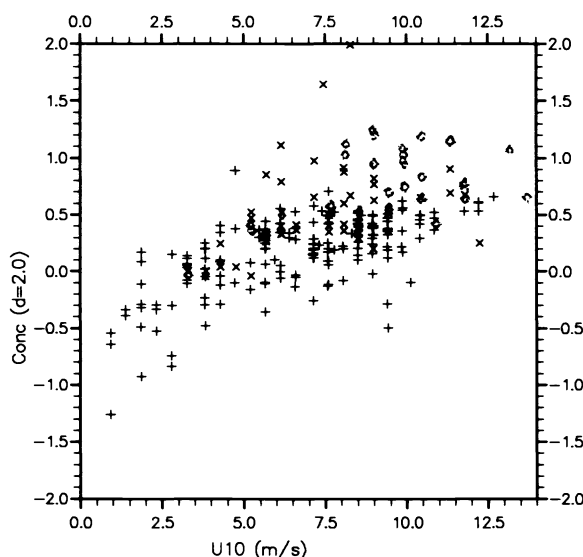


Figure 1. Concentrations of aerosol particles of  $2 \mu\text{m}$  in diameter ( $C_{80}(D=2.0 \mu\text{m})$ ) as function of 10-m wind speed. Note that the aerosol concentrations have been plotted on a logarithmic scale with a dynamic range of four decades. No selection has been made for the aerosol concentrations, i.e. all data are included (see section 2 for selection criteria). Three ASTD cases (see text) have been plotted with different symbols: + for  $ASTD < 0$ ; X for  $0 < ASTD < 0.5$ ; ◇ for  $ASTD > 0.5$ .

2  $\mu\text{m}$  in diameter. The increase of the particle concentrations with wind speed is in accordance with their marine origin and the increased production by breaking waves and more efficient mixing as wind speed increases (cf. Van Eijk and De Leeuw<sup>8</sup> for a brief discussion). Smith et al.<sup>14</sup> also observed that in purely marine air masses the concentrations increase with wind speed. The wind speed dependence increases with increasing particle diameter, as indicated in Figure 2a, where the data from the North Atlantic are presented by X. The extrapolated zero-wind-speed concentrations are presented in Figure 2b. Curves II and VII in Figure 2 were taken from Van Eijk and De Leeuw<sup>8</sup> and represent data from the North Sea at Meetpost Noordwijk in wind directions 155°-190° and 285°-310°, respectively. Together these data sets constitute three different fetches, i.e. about 20 km (curve II), about 200 km (curve VII) and an "infinite" fetch for the present data. We see that the wind speed dependence is similar for the largest particles. The differences between curves II and VII for particles smaller than about 4  $\mu\text{m}$  have previously been explained by a larger relative contribution of continental particles at the shortest fetch (curve II). The concentration of continental particles decreases faster due to turbulent deposition and faster dispersion as the wind speed increases. The intercepts in the regression lines for the North Atlantic data are seen to be somewhat lower for particles of about 2  $\mu\text{m}$ , and higher for larger particles, as compared with the North Sea data. The three curves intersect at a diameter of about 2  $\mu\text{m}$ . Apparently, this particle size divides particles of continental and marine origin.

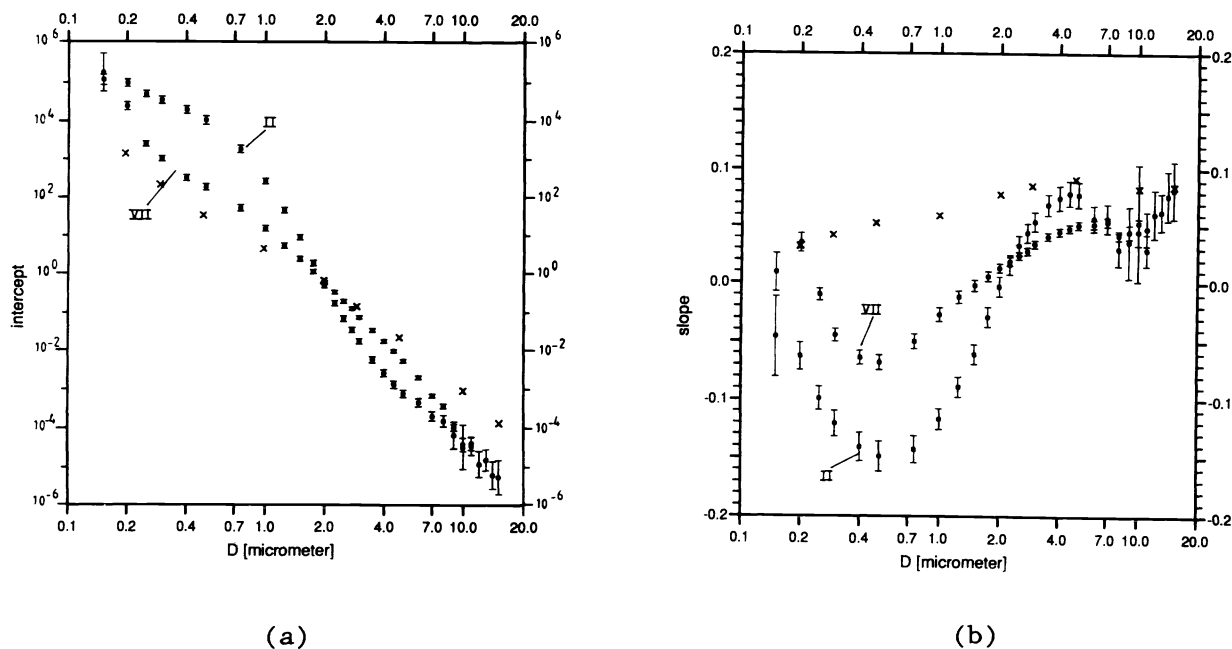


Figure 2. Intercepts and slopes (a and b in eq. 3) of  $C_{80}(D)$  versus  $u_{10N}$  plots as a function of diameter  $D$ . Note that the intercepts are the  $^{10}\log$  of the extrapolated zero-wind-speed concentrations. The present data are presented by X; curves II and VII were taken from Van Eijk and De Leeuw<sup>8</sup> and represent data from the North Sea at Meetpost Noordwijk in wind directions 155°-190° and 285°-310°, respectively. The three data sets are for different fetches for industrial polluted air masses (II and VII) and clean open-ocean air masses (see text).

The data in Figure 2 can be used to construct a model for the aerosol particle size distribution as function of wind speed. Because the wind-speed dependence increases with particle size, the shape of the particle size distribution obviously also changes with wind speed.

**24-Hour averaged wind speed.** In NAM the differences in wind speed dependence of small and large particles are accounted for by parameterization of the aged marine mode ( $D_{20} = 0.48 \mu\text{m}$ ) in terms of the 24-hour average wind speed ( $\langle u \rangle_{24}$ ), while the amplitude of the fresh marine mode ( $D_{30} = 4 \mu\text{m}$ ) is determined by the current wind speed. Regression of our open ocean data on  $\langle u \rangle_{24}$  leads to some improvement in the correlation coefficients for  $D \leq 0.5 \mu\text{m}$ , but the regression coefficients are similar to those in Figure 2. Hence the use of the 24-hour average wind speed does not lead to a parameterization of our open-ocean data which is different from a parameterization based on the current wind speed.

**Wind direction.** In the middle of the North Atlantic where we took our measurements, the fetch is so long that influences of aerosol generated over land, as observed over the North Sea,<sup>8</sup> are expected to be negligible. Moreover, the air mass trajectories and Radon concentrations indicate that the air masses had been over water during at least three days. Nevertheless, the data set was partitioned into four sectors (north, east, south and west) because of the different meteorological properties of air masses of arctic and tropical origin. In arctic air masses the air was generally colder than the sea, leading to slightly unstable stratification, while in tropical air masses the air was generally somewhat warmer than the sea resulting in stable stratification. In the latter case, the air was also more humid and the cooling by interaction with the surface led to saturation resulting in fog near the surface or drizzle. The partitioning in four wind sectors led to appreciable increases of the correlation between the particle concentrations and  $u_{10N}$ , while at the same time the regression coefficients often changed as well. This leads to the conclusion that even in purely marine air masses synoptic scale effects must be taken into account and can lead to significant improvement of the parameterization. On the other hand, since also the micro-meteorological properties change with the type of air mass, other parameters such as the thermal stability or ASTD might be used for the parameterization instead of the applied partitioning in wind sectors. This will be investigated below.

**Thermal stability (ASTD).** The thermal stability, further expressed as the ASTD, has an appreciable effect on the whitecap ratio (W) and therefore also on the aerosol production rate.<sup>1</sup> In unstable situations (ASTD < 0) more whitecapping occurs, and W increases as the ASTD becomes more negative. Thus also the aerosol production rate increases. However, at the same time thermal mixing also increases and disperses the aerosol throughout the boundary layer, leading to dilution near the surface. These two processes have opposing effects on the low-level concentrations: on the one hand more aerosol is produced, while on the other it is faster dispersed.

The reverse applies in stable situations: W decreases with increasing ASTD and therefore also the production rate decreases. On the other hand, the stable stratification prohibits mixing and the aerosol is confined to a thin layer near the surface.

We considered three cases in our analysis:

- a. unstable to neutral                      ASTD < 0,

- b. neutral to stable    0 < ASTD < 0.5
- c. stable                0.5 < ASTD

The effect of the ASTD is very obvious in scatterplots of  $C_{80}(D)$  versus  $u_{10N}$ . Concentrations measured in stable conditions are higher than those collected in neutral or unstable conditions. The range of wind speeds is similar for each case, but the number of data points in cases b and c was much smaller than for case a. This influences the statistical reliability. In the plot of the particle concentrations as function of  $u_{10N}$  in Figure 1, the three stability cases have been indicated with different symbols. The regression of the particle concentrations on  $u_{10N}$  yielded similar results for the first two cases, but in the stable situation the wind speed dependence was about a factor two larger. Since the effect of mechanical turbulent mixing is independent of ASTD, the stronger wind speed dependence in the stable situation is ascribed to the smaller mixing depth. The smaller (extrapolated) zero-wind-speed concentration in the stable situation (intercept=0.42, as compared to 0.60 and 0.65 in cases a and b, respectively) is ascribed to the smaller production rate.

For the final analysis of the effect of ASTD on the aerosol concentrations, we first removed the wind speed effect because it dominates the aerosol concentrations and obscures effects of other parameters:<sup>8</sup>

$$C_{rel}(D) = C_{80}(D)/M_{80}(D), \tag{7}$$

where  $M_{80}(D)$  is the concentration estimated from  $u_{10N}$  (see Figure 2). The relative concentrations  $C_{rel}(D)$  were correlated on ASTD. Correlation coefficients vary from 0.05 to 0.60. Introduction of the obtained relations into the model leads to a small increase in the performance (5-7%).

Comparison of the two methods used to analyse the effect of ASTD on the aerosol concentrations (i.e. wind direction versus ASTD intervals) shows that the best results are obtained when considering the wind speed dependence in ASTD intervals.

**Water temperature.** The variation in the water temperature during this experiment was too small to have a significant effect. Regression of  $C_{rel}(D)$  on the water temperature resulted in correlation coefficients smaller than 0.15.

### 3.2 Extinction

Extinction coefficients at 0.55, 0.69, 1.064, 4.0 and 10.6  $\mu\text{m}$  were directly correlated with meteorological parameters. Humidity corrections, as applied to the aerosol concentrations, are not possible. Therefore, these effects were estimated from the statistical analysis (see below). In the regression analyses the Chauvenet criterion (eq. 4) has been applied.

**Wind speed.** Due to the increase of the aerosol concentrations with wind speed, for all sizes in this open ocean case (see Figure 2b), also the extinction coefficients increase with wind speed. Correlation coefficients are 0.67-0.78. The regression lines predict the extinction coefficients within a factor of 1.6! Wind speed effects dominate all other effects for the cases considered, i.e. when fog and rain are excluded from the analysis.

**ASTD.** The effect of ASTD on the extinction coefficients was determined after correction for the effects of wind speed. Here we only used the relative extinction

method, which was calculated similarly as the relative aerosol concentrations (see eq. 7). Regression of the relative extinction coefficients on the ASTD yielded correlation coefficients of 0.46-0.54. Introduction of the effects of ASTD into the extinction model yielded a small increase of the performance.

**Relative humidity.** The effects of the relative humidity on the extinction coefficients, for RH<96%, are also obscured by wind speed effects. The relative extinction coefficients increase with relative humidity and correlation coefficients between these parameters of 0.38-0.46 were obtained. Inclusion of the humidity effects in the model has only a minor effect on the performance.

**Water temperature.** Correlations between the relative extinction coefficients and the water temperature are negligible, as in the case for the aerosol concentrations. The variations in the water temperature (11-13°C) during this field experiment were too small to expect a significant effect. Nevertheless, this parameter has been included because of the effect it may have on the production rate and because significant differences have been observed between concentrations of large aerosols in cold and warm water.<sup>15</sup>

#### 4. MODEL COMPARISON

The two models presented above were formulated to calculate the extinction coefficients at the wavelengths of interest based on observations of simple meteorological parameters. For the aerosol model, first the aerosol particle size distributions were determined from the meteorological parameters and subsequently the extinction coefficients were calculated using the exact Mie code (see also ref. 10). The results were evaluated by comparison with the extinction coefficients that were calculated with the exact Mie code from the measured particle size distributions, further denoted as "experimental extinction coefficients" or  $\alpha_{\text{exp}}$ .

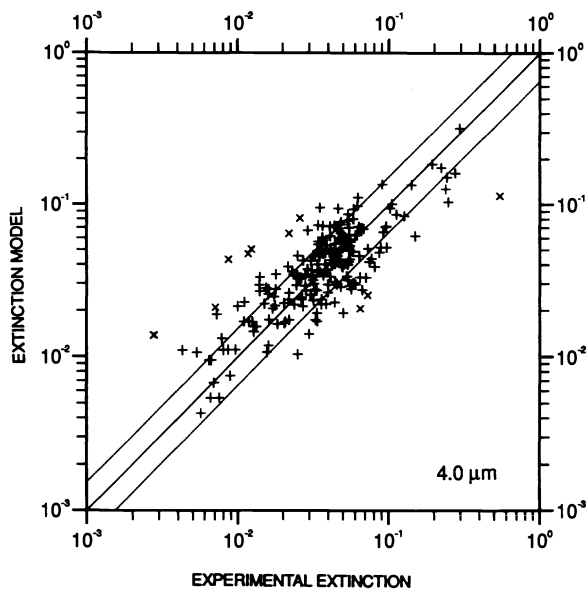
A similar comparison has been made of extinctions calculated from the meteorological parameters using the extinction model. As an example, results of the latter comparison are shown in Figure 3a, for a wavelength of 4  $\mu\text{m}$ .

The performance of the models can be assessed from the standard deviation  $\sigma_{y=x}$  of the regression between the modelled extinction coefficients (y) and  $\alpha_{\text{exp}}$  (x) with respect to the identity line  $y=x$  (ideal model performance). The value of  $\sigma_{y=x}$  is a measure for the factor F to within the model predicts  $\alpha_{\text{exp}}$  (68% confidence limit). Since  $\sigma_{y=x}$  is determined from scatterplots of the logarithms of the extinction coefficients, F is given by:

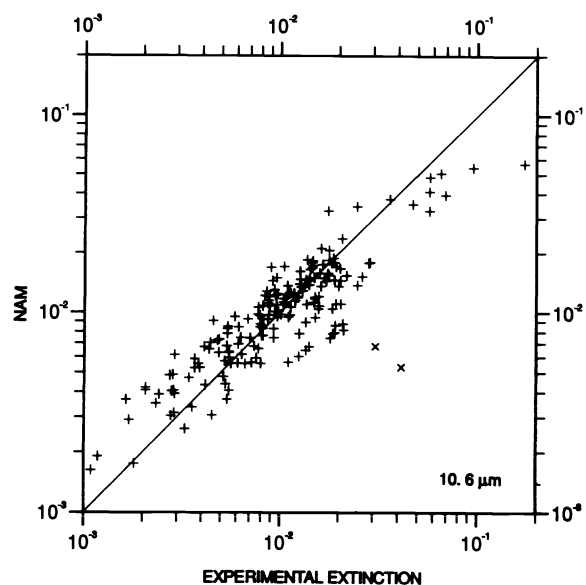
$$F = 10^{\sigma_{y=x}} \quad (8)$$

The results of this model performance analysis are presented in table 1. Obviously, the direct extinction model yields better results in this area where the aerosol is of purely maritime origin and continental contributions are negligible.

Also included in table 1 is the performance analysis for NAM, based on two estimates for the visibility. The first, NAM(AEG) is based on a visibility measurement with an AEG point visibility meter. Because during the experiments the visibility was usually very good, the AEG point visibility meter was often pegged at its maximum value of 40 km. In these cases the NAM prediction could not be based on



(a)



(b)

Figure 3. Comparison of modelled and experimental extinction coefficients ( $\alpha_{\text{exp}}$ ):  
 a. extinction coefficients calculated from the extinction model (section 3.2) for a wavelength of  $4 \mu\text{m}$   
 b. NAM extinction coefficients at  $10.6 \mu\text{m}$  calculated with visibilities derived from the aerosol extinction at  $0.55 \mu\text{m}$  (eq. 9).

the visibility. Also an estimate of the air mass parameter based on Radon was not useful because the Radon counts were very low and showed very little variation. As mentioned before, the air mass trajectory analysis always indicated a purely marine air mass which had resided over the ocean since at least 72 hours. As a result, the variations in the NAM prediction were mainly caused by wind speed and humidity variations, while the small-particle mode had no effect except in the few cases when the visibility was smaller than 40 km.

As an alternative, we used the visibility calculated from the  $0.55 \mu\text{m}$  extinction coefficient:

$$\text{VIS} = 3.195 / \alpha(0.55 \mu\text{m}) \quad (9)$$

Using these values, very good performance of NAM was obtained as compared with the experimental values  $\alpha_{\text{exp}}$ . The results are presented in the last column in table 1. The decrease of the standard deviations at shorter wavelengths is of course due to the use of a visibility derived from the extinction coefficient at  $0.55 \mu\text{m}$  where in this special case the expected perfect fit is observed. A comparison between the NAM predicted extinction coefficients at  $10.6 \mu\text{m}$  and  $\alpha_{\text{exp}}$  is presented in Figure 3b.

Table 1. Performance assessment of extinction models

wavelength	aerosol model		extinction model		NAM(AEG)		NAM( $\sigma_{0.55}$ )	
	$\sigma$	F	$\sigma$	F	$\sigma$	F	$\sigma$	F
10.6	0.28	1.9	0.18	1.5	0.22	1.7	0.16	1.4
4.0	0.37	2.3	0.18	1.5	0.25	1.8	0.20	1.6
1.064	0.35	2.2	0.17	1.5	0.25	1.8	0.13	1.3
0.69	0.35	2.2	0.15	1.4	0.24	1.7	0.05	1.1
0.55	0.35	2.2	0.15	1.4	0.27	1.9	0.00	1.0

## 5. DISCUSSION

Two models have been derived from a statistical analysis of particle size distributions and calculated extinction coefficients in the purely marine atmosphere of the North Atlantic. Comparison of these models with experimental extinction coefficients shows that the direct extinction model is superior to the aerosol model. Using the extinction model, the extinction coefficients in the visible and IR bands can be predicted with an accuracy of a factor 1.5. With the aerosol model the accuracy is a factor of 2.2. The latter figure is similar to that derived from the performance analysis of the aerosol model that was previously derived for the North Sea.<sup>10</sup>

The comparison with the performance of NAM in the IR bands shows that our extinction model yields similar accuracy. However, NAM has been used with visibility values that were derived from the measured aerosol particle size distributions. With the observed visibility the performance of NAM degrades. In general, a reliable observation of the visibility must be used to obtain an accurate extinction coefficient from NAM.

On the other hand, the performance of the present extinction model has been evaluated with the same data that were used to formulate the model. An honest evaluation requires that an independent data set is used.

The aerosol model is believed to be more generally applicable than the extinction model. Although it is strictly an empirical model, is based on aerosol physics. This also applies to NAM. The present analysis shows that NAM performs excellent in this purely marine environment. This is in contrast with results obtained from the North Sea, where the performance of NAM was poor in off-shore winds.<sup>10</sup> In the latter case the North Sea aerosol model<sup>8</sup> yielded much better results.

The alternative of modeling the extinction coefficients directly from the meteorological parameters is attractive because of simplicity. However, much physical detail will be lost and effects of changes in the particle size distributions due to meteorological effects and influences of different sources cannot easily be taken into account.

## 6. ACKNOWLEDGEMENTS

The research described in this paper was carried out under contracts A90KM638 and A92KM615 from the Netherlands Ministry of Defence.

## 7. REFERENCES

1. E.C. Monahan, "The ocean as a source for atmospheric particles," The role of air-sea exchange in geochemical cycling, P. Buat-Menard (Ed.), 129-163, Reidel, Dordrecht, 1986.
2. G. de Leeuw, "Modeling of extinction and backscatter profiles in the marine mixed-layer," *Appl. Opt.* 28, 1356-1359, 1989.
3. S.G. Gathman, "Optical properties of the marine aerosol as predicted by the Navy aerosol model," *Opt. Eng.* 22, 57-62, 1983.
4. S.G. Gathman, "A preliminary description of NOVAM, the Navy Oceanic Vertical Aerosol Model," Naval Research Laboratory, Washington D.C., U.S.A., NRL Report 9200, 1989.
5. F.X. Kneizys, E.P. Shettle, L.W. Abreu, J.H. Chetwynd Jr., G.P. Anderson, W.O. Gallery, J.E.A. Selby and S.A. Clough, "Users guide LOWTRAN 7", AFGL-TR-88-0177, 1988.
6. G. de Leeuw, K.L. Davidson, S.G. Gathman and R.V. Noonkester, "Modeling of aerosols in the marine mixed-layer," Propagation Engineering, Proc. SPIE 1115, pp. 287-294, 1989.
7. S.G. Gathman, G. de Leeuw, K.L. Davidson and D. Jensen, "The Naval Oceanic Vertical Aerosol Model: Progress Report," Atmospheric propagation in the UV, visible, IR and mm-wave region and related systems aspects, AGARD-CP-454, pp. 17-1 to 17-11, 1990.
8. A.M.J. van Eijk and G. de Leeuw, "Modeling aerosol particle size distributions over the North Sea," *J. Geophys. Res.* 97 (C9), pp. 14417-14429, 1992.
9. G. de Leeuw, "Aerosol models for optical and IR propagation in the marine atmospheric boundary layer," Propagation Engineering: Fourth in a series, L.R. Bissonnette and W.B. Miller (Eds.), Proc. SPIE 1487, 130-159, 1991.
10. A.M.J. van Eijk and G. de Leeuw, "Modeling aerosol extinction in a coastal environment," Atmospheric Propagation and Remote Sensing, A. Kohnle and W.B. Miller (Eds.), Proc. SPIE 1688, 28-36, 1992.
11. W.T. Liu, K.B. Katsaros and J.A. Businger, "Bulk parameterization of air-sea exchanges of heat and water vapor including the molecular constraints at the interface," *J. Atmos. Sci.* 36, 1722-1735, 1979.
12. J. Wierenga, "Gust factor over open water and build up country," *Boundary Layer Meteorol.*, 3, 424-441, 1973.
13. J.W. Fitzgerald, "Approximation formulas for the equilibrium size of an aerosol particle as a function of its dry size and composition and the ambient relative humidity," *J. Appl. Meteor.* 14, 1044-1049, 1975.
14. M.H. Smith, I.E. Consterdine and P.M. Park, "Atmospheric loadings of marine aerosol during a Hebridean cyclone," *Q. J. R. Meteorol. Soc.* 115, 383-395, 1989.
15. G. de Leeuw and G.J. Kunz, "NOVAM evaluation from aerosol and lidar measurements in a tropical marine environment," Atmospheric Propagation and Remote Sensing, A. Kohnle and W.B. Miller (Eds.), Proc. SPIE 1688, 14-27, 1992.
16. G. de Leeuw, M.M. Moerman and L.H. Cohen, "Survey of aerosol and lidar measurements at the North Atlantic (25 May-28 June, 1983)," Physics Laboratory TNO, report PHL 1984-01, 98 pp., 1984.